

1 Electrochemically enhanced simultaneous degradation of
2 Sulfamethoxazole, Ciprofloxacin and Amoxicillin from aqueous solution
3 by multi-walled carbon nanotubes filter

4

5 Ting-Yuan Tan ^{a, 1}, Zhuo-Tong Zeng ^{b, 1}, Guang-Ming Zeng ^{a, *}, Ji-Lai
6 Gong ^{a, *}, Rong Xiao ^{a, *}, Peng Zhang ^a, Biao Song ^a, Wang-Wang Tang ^a,
7 Xiao-Ya Ren ^a

8 ^a College of Environmental Science and Engineering, Hunan University and Key Laboratory of
9 Environmental Biology and Pollution Control (Hunan University), Ministry of Education,
10 Changsha 410082, PR China;

11 ^b Department of Dermatology, Second Xiangya Hospital, Central South University, Changsha
12 410011, P R China.

13

14

15 * Corresponding authors:

16 zgming@hnu.edu.cn (G. Zeng); jilai@gong@hnu.edu.cn (J. Gong); xiaorong65@csu.edu.cn (R.
17 Xiao)

18 ¹ These authors contributed equally to this article.

19

Accepted MS

20 **Abstract**

21 Electrochemical filters exhibited excellent properties of time saving and energy
22 conservation and were widely used in water purification. In this work, an efficient
23 method was proposed for degrading antibiotics including sulfamethoxazole (SMZ),
24 ciprofloxacin (CIP) and amoxicillin (AMO) in both single system and mixed system
25 by utilizing multi-walled carbon nanotubes (MWCNTs)-based electrochemical
26 membrane. The effect of experimental parameters was investigated with respect to
27 voltage, pH, temperature, initial pollutant concentration and sodium dodecyl benzene
28 sulfonate (SDBS). The recycling experiments of MWCNTs-based electrochemical
29 filter were also performed. Results revealed that the degradation efficiency could be
30 enhanced by increasing the voltage and temperature, while it decreased with the
31 increased initial pollutant concentration and the addition of SDBS. Degradation of
32 SMZ and AMO was weakly affected by solution pH. However, the degradation
33 efficiency of CIP in acidic or alkaline solution was much higher than that in neutral
34 solution. Furthermore, the MWCNTs-based electrochemical membrane still exhibited
35 high efficiency for antibiotic degradation after reuse of four times, which could
36 facilitate the development of reproducible and low-cost pollutant-processing method.
37 Noticeably, this membrane filter also presented high performance on simultaneously
38 removing the multiple antibiotics with the efficiency order of AMO (98%) > SMZ
39 (95%) > CIP (29%). The degradation mechanism of antibiotics by the
40 MWCNTs-based membrane was analyzed and a clear explanation on the
41 antibiotics-removed pathway was provided. These results indicated that the
42 MWCNTs-based electrochemical membrane filtration may have potential to
43 effectively treat multiple antibiotics in real wastewater.

44 **Keywords:** Multi-walled carbon nanotubes, Multiple antibiotics, Reaction products,
45 Oxidation mechanisms

46 1. Introduction

47 Much effort are being made for purifying the waste water due to the massive
48 industry-discharged inorganic/organic pollutants such as, chemicals, dyes, drugs and
49 pesticides [1-3]. Due to the characteristics of complex structure, high strength, hard
50 degradation, and high activity of their metabolites, antibiotic drugs released to
51 aqueous environment inevitably cause water pollution [4, 5]. Therefore, antibiotics
52 have put some challenges for waste water treatment, thus posing potential hazards to
53 environment and health [6]. The types and concentrations of antibiotics in the aquatic
54 environment are not the same for different countries and modes of use. Europe
55 presents a north-south gradient, with usage in the north (Finland, Slovakia, etc.)
56 significantly lower than in the south (Italy, Spain, etc.) [7]. However, there are
57 significant east-west differences in China, with the average emission density of
58 antibiotics in the eastern cities being 6 times that of the western cities [8]. According
59 to reports, in 2013, the ratio of sulfonamides, quinolones and β -lactam antibiotics in
60 Europe was 2.9%, 8.3% and 11.3%, respectively. However, their ratios in China are
61 5%, 17% and 21%, respectively [7, 8]. Globally, the detection range of antibiotics has
62 reached from ppm to ppt levels, even after the wastewater treatment plants (WWTPs).
63 In Europe, including Croatia, Germany and Portugal, the concentration of
64 sulfonamides after WWTPs was approximately 2 $\mu\text{g/l}$ [7]. In Asia, quinolones and
65 sulfonamides were found after WWTP in Beijing, with an average concentration of 5
66 and 3 $\mu\text{g/L}$, respectively [9]. In South Korea, tetracycline and sulfonamides after
67 WWTP are also at ppb levels [10]. However, it is well known that organisms in the
68 environment are generally not exposed to a single compound but are exposed to a
69 mixture of antibiotics [11]. Leung et al. reported that 89% of 113 samples of tap water
70 in 13 Chinese cities contained 17 drugs [12]. Therefore, it is necessary and urgent to
71 simultaneously remove multiple antibiotics and their conversion products.

72 **Traditional methods for removing antibiotics in water include coagulation,**
73 **adsorption, and biological systems. They have certain limitations. A disadvantage of**
74 **these conventional processes is that they do not real degrade the contaminants but**

75 concentrate and transfer them to produce new waste that requires subsequent
76 processing to remove the new waste [13, 14]. Hence, various new technologies have
77 been subsequently studied to degrade antibiotics. Advanced oxidation processes based
78 on electrochemical technology have attracted more and more attention as an
79 alternative for traditional methods [15-17].

80 Electrochemical oxidation refers to generating free radicals through a series of
81 reactions in a certain container, such as solvated electron, $\bullet\text{OH}$, $\bullet\text{O}_2$, and $\text{Cl}\bullet$ on the
82 anode. These free radicals can decompose pollutants and the process is irreversible.
83 Usually this method is also seen as a greener alternative to other approaches [18].
84 Several electrode materials were tested for the degradation of amoxicillin (AMO), the
85 study showed that BDD had proven to be the best anode material at high current
86 densities, forming a large number of hydroxyl radicals and other oxidants such as
87 hydrogen peroxide, which contributed to the enhancement of oxidation and
88 mineralization of AMO [19]. Recently, ceramic electrodes based on
89 sub-stoichiometric titanium oxides, particularly Ti_2O_3 was systematically studied for
90 degradation and mineralization of AMO [20]. However, the strict conditions, not
91 enough efficiency and high operating costs due to high energy consumption were still
92 the main drawbacks limiting the large-scale application of electrochemical processes.
93 For example, the antibiotic amoxicillin was completely mineralized with BDD anodic
94 Fenton, but the pH requirement was strong acid [21]. Homem et al. summarized that
95 direct oxidation efficiency depended on the catalytic activity of the electrode, the
96 diffusion rate of the anode active compound and the current, while the indirect
97 oxidation was strongly dependent on the diffusion rate of the oxidizing agent in the
98 solution, the temperature and pH [22]. In the electrochemical cell amoxicillin
99 elimination was only 80% after 240 minutes of degradation [23]. Therefore, it is an
100 urgent need to further improve the degradation efficiency of antibiotics using new
101 approaches.

102 Membrane filtration technologies were efficient ways of removing water
103 micro-pollutants [24]. There have been some studies on the removal of
104 micro-pollutants in water by carbon nanotube membranes. Wang et al. have studied

105 the pre-coagulation of wastewater by filtration through carbon nanotube membranes
106 to remove acetaminophen, triclosan, caffeine and carbendazim [25]. Hybrid carbon
107 membrane also was studied to remove tetracycline antibiotics in water [26].
108 Nanocomposite membranes containing single-walled and multi-walled carbon
109 nanotubes (SWCNTs and MWCNTs) have been reported for the filtration of triclosan,
110 acetaminophen and ibuprofen [27]. Acid-treated carbon nanotubes and Polyvinyl
111 chloride (PVC) polymeric ultrafiltration membranes were also reported to remove
112 bisphenol A and norfloxacin from drinking water [28]. Although membrane filtration
113 has been used to remove more complex contaminants, it still was dependent on initial
114 concentration, ionic strength, pH, membrane fouling and transmembrane pressure are
115 challenges for membrane filtration [29].

116 Compared to conventional filtration systems, electro-catalytic membranes with
117 higher removal efficiencies can provide the removal of the target pollutants by both
118 adsorptive filtration and electrochemical degradation under applied voltage, thus
119 avoiding time-consuming requirements and lowering energy consumption [30].
120 Carbon nanotubes (CNTs) were a new type of porous structure adsorbents with good
121 electrical conductivity and strong interaction with contaminants [31]. **There were**
122 **some studies have summarized coupling of membrane filtration and advanced**
123 **oxidation processes for removal of pollutants [32, 33].** CNTs-based electro-catalytic
124 membranes with appropriate size and configuration pores possessed three times
125 higher performance than that of conventional polymeric electro-catalytic membranes
126 without well-defined pores [34]. In addition, CNTs-based electro-catalytic membranes
127 exhibited stable, conductive and porous three-dimensional networks for enhanced ion
128 and molecular transport [35]. Liu reported that main mechanism of electrochemical
129 membrane filtration depended on mass transfer, physical adsorption and electron
130 transfer [36]. Recently, it was reported that carbon nanotube based filters use
131 electrochemical catalysis to degrade pollutants. The first discovered electrochemical
132 MWCNTs filter was used as a drinking water purification technology for pathogen
133 removal and inactivation, whereby the application potential was developed [37]. A
134 significant removal of bisphenol A with identical performance was also reported using

135 both pristine and boron-doped MWNTs-based filters [38]. Results showed that
136 oxidation reaction dominates at a higher voltage (2-3 V) and surface adsorption
137 played an important role under a lower voltage (0-1 V) [38]. Noticeably, CNT
138 network cathode filter was developed to remove antibiotic tetracycline. Compared
139 with perforated Ti cathode filter, CNT network filter is performed at a lower cell
140 voltage to achieve similar performance, thus greatly reducing energy consumption
141 [39]. Tetracycline was also degraded using a Nano-TiO₂/carbon electro-catalytic
142 membrane. It was found that the removal efficiency for tetracycline was almost
143 independent on pH value and tetracycline was completely removed at the
144 concentration of 50 mg/L [40]. A conductive cellulose-based anion electrochemical
145 filter was documented by incorporating CNT as fillers to remove ferrocyanide, methyl
146 orange and antibiotic tetracycline [41]. Moreover, results showed that the maximum
147 electrooxidation flux was 0.9 mol/h/m² for 0.2 mmol/L tetracycline [41]. In the
148 cross-flow filtration mode combined with electrochemical oxidation, the effects of
149 permeate flux, contaminant concentration and current density on the mineralization
150 efficiency of various organic compounds (oxalic acid, acetaminophen, phenol) were
151 systematically evaluated [42]. The removal mechanism of p-nitrophenol,
152 p-methoxyphenol and p-benzoquinone on the porous Ti₄O₇ reaction electrochemical
153 membrane under anodic polarization was also investigated, which indicated that •OH
154 was mainly formed by electrochemical reaction [43]. The perusal of the literature
155 indicated that CNT-based electrochemical membrane filtration was applied for
156 removing only single antibiotic in wastewater. No literature was reported on the
157 application of electrochemical CNT-based membrane filtration to remove multiple
158 antibiotics in wastewater.

159 In this study, an electrochemical membrane filter was fabricated using MWCNTs
160 as anode and perforated stainless steel as cathode for simultaneous removal of
161 multiple antibiotics including sulfamethoxazole (SMZ), ciprofloxacin (CIP) and
162 amoxicillin (AMO). We studied on the application of electrochemical CNT-based
163 membrane filtration to degrade antibiotics in wastewater. And we systematically
164 studied the simultaneously removal of multiple antibiotics. Background curve and

165 breakthrough curves were completed to investigate electron transfer and sorption
166 processes, respectively. Experimental factors that influence the degradation efficiency,
167 such as voltage, pH, temperature, concentration, sodium dodecyl benzene sulfonate
168 (SDBS), recyclability were investigated. Mixed pollution systems included binary
169 mixture (i.e., SMZ + CIP, SMZ + AMO, CIP + AMO) and ternary mixture (i.e., SMZ
170 + CIP + AMO). The electrochemical mechanism and the degradation products were
171 also investigated.

172 2. Materials and methods

173 2.1 Chemicals and materials

174 Sodium chloride (purity $\geq 99.5\%$, NaCl) was purchased from Tianjin Fengchuan
175 Chemical Reagent Technologies Co. Ltd. SMZ (purity $\geq 99\%$, $C_{10}H_{11}N_3O_3S$), CIP
176 (purity $\geq 99\%$, $C_{17}H_{18}FN_3O_3$) and AMO (purity $\geq 99\%$, $C_{16}H_{19}N_3O_5S$) were
177 obtained from Sigma-Aldrich. Porous MWCNTs (purity $\geq 95\%$, $d = 750$ nm and $l =$
178 $10-20$ μ m) were purchased from Chengdu Organic Chemistry Co., Chinese Academy
179 of Sciences, China. Ultrapure water (18.2 M Ω ·cm, produced by Barnstead
180 SMART2PURE system, ThermoFisher Scientific) was used throughout the whole
181 experiments.

182 The MWCNTs powders were dispersed in dimethyl formamide (DMF) and probe
183 sonicating for 15min (ultrasound time was 3s, interval time was 4s, power was 400W).
184 Then, the obtained MWCNTs dispersion was filtered onto a 5 μ m Poly tetra
185 fluoroethylene (PTFE) membrane under vacuum condition. The MWCNTs membrane
186 was washed with 100 mL of ethanol, 250 mL of ultrapure water to remove DMF
187 before use, resulting in filter loading area was 706 mm². NaCl was used as the
188 background electrolyte (20 mM) to normalize ionic strength and conductivity, the
189 influent concentration was 5 mg/L.

190 2.2 MWCNTs Electrochemical Filtration Setup

191 All filtration experiments were achieved using the improved electrochemical
192 filtration casing as shown in Fig. 1 a and b. A porous MWCNTs network was put on a
193 PTFE membrane (filtration area=706 mm²) and laid into the improved
194 electrochemical filtration casing. Cathode was composed of a stainless steel network.

195 Anode was stainless steel network combined with porous MWCNTs network which
196 were coated on PTFE membrane. Insulating Si-rubber O-ring with 1 cm thickness was
197 used to seal and separate the electrodes. In order to strengthen the conductivity, the
198 anodic stainless steel network was put onto the MWCNTs network. Typically, the
199 influent flowed first through cathodic porous stainless steel networks, followed by
200 anodic porous stainless steel networks, and finally an anodic MWCNTs network and
201 PTFE membrane.

202 **2.3 Characterization**

203 The Background curve was implemented to characterize electrochemical
204 properties. A three-electrode system was used in this study including MWCNTs
205 working electrode, Ag/AgCl reference electrode, and a stainless steel wire counter
206 electrode. This measurement was completed by an electrochemical workstation (CHI
207 660D, Shanghai Chenhua Instrument Co. Ltd., China). The surface morphology of the
208 membrane was determined by scanning electron microscopy (SEM).

209 **2.4 Breakthrough Curve Measurement**

210 In the absence of a power source, a breakthrough curve experiment was
211 performed. The influent concentration was 5 mg/L and effluent aliquots were
212 collected every 3 min until the effluent concentration was equal to the influent
213 concentration.

214 **2.5 Evaluation of MWCNTs electrochemical filtration performance**

215 In this study, three different antibiotics including SMZ, CIP and AMO were
216 chosen to evaluate the filtration performance of MWCNTs electrochemical filtration
217 membrane. The filtration experiments of different antibiotics were executed by a
218 syringe filter. A syringe pumped ultrapure water at a speed of 1.5 mL/min to flush and
219 calibrate the flow.

220 The effect of experimental parameters including antibiotic concentrations (i.e., 5
221 mg/L, 25 mg/L and 50 mg/L), voltages (i.e., 0 V, 1 V, 2 V and 3 V), pH values (3, 5, 7,
222 9 and 11) and temperatures (15 °C, 25 °C and 35 °C) were investigated. The effect of
223 SDBS with a concentration of 5 mg/L on degradation efficiency was also investigated.
224 MWCNTs filter was washed by ethanol under vacuum condition after membrane

225 filtration for further use.

226 Moreover, the mixed antibiotics solutions (i.e., binary system and ternary system)
227 filtration experiments by MWCNTs-based electrochemical membrane filtration were
228 also performed at 25 °C. In the binary or ternary system, the concentration of each
229 antibiotic was fixed at 5 mg/L. The total filtration volume was 100 mL. The effluent
230 was collected every 5 min and analyzed by high performance liquid chromatography
231 to confirm the target effluent concentration.

232 **2.6 Analytical methods**

233 The effluent was collected at given time intervals and its concentration was
234 measured by an HPLC Series 1100 (Agilent, Waldbronn, Germany) equipped with a
235 diode array detector (DAD). Noticeably, the effluent was first filtered by 0.22 µm
236 membrane filter with subsequent concentration analysis. The column was a C-18
237 column (4.6 × 250 mm) at the temperature of 40 °C. The mobile phase was a mixture
238 of acetonitrile (A) and 0.1% v/v formic acid (B) at the flow rate 1 mL/min. Gradient
239 elution was performed using 5% A and 95% B for 8.0 min, followed by 15% A and 85%
240 B for 12.0 min, and an equilibration time of 2 min and then back to initial value in 4
241 min. The sample volumes for injection were all 20 µL and the wavelength of detector
242 was 275 nm (SMZ and CIP) and 228 nm (AMO). Under these conditions, the
243 retention times of SMZ, CIP, and AMO were 4.3, 7.9 and 24.7 min, respectively.

244 A liquid chromatography mass spectrometry (LC-MS) (Agilent 1290/6460,
245 Triple Quad MS, USA) was used to determine the intermediate products from SMZ,
246 CIP and AMO degradations. For SMZ, the mobile phase was composed of acetonitrile
247 (solvent A) and 0.1% formic acid dissolved in water (solvent B) in gradient flow. The
248 elution program (mobile phase) for LC-MS analysis is as follows: from initial to 1
249 min, solvent A and B was used in the ratio of 10:90 (A:B = 10:90); from 2 min to 6
250 min, A:B = 40:60; from 7 min to 12 min, A:B = 60:40; from 13 min to 16 min, A:B =
251 80:20 and from 17 min to 20 min, A:B = 10:90, respectively. For CIP, the mobile
252 phase composition was acetonitrile (A) and water containing 0.1% formic acid (B) at
253 a flow rate of 0.25 mL/min. the mobile phase composition (A/B) started at 10/90 (v/v)
254 with a linear increase to 90/10 (v/v) in 7 min, where it was held for 4 min. Then the

255 gradient was returned to 10/90 (v/v) and kept for 5 min to allow for equilibration. For
256 AMO, the mobile phase consisted of a mixture of solution A (0.1% formic acid in
257 water) and solution B (0.1% formic acid in acetonitrile) with an initial composition of
258 90% solution A and 10% solution B. The mobile phase composition changed linearly
259 from 10% solution B to 40% at 10.0 min, then solution B was re-equilibrated to
260 starting conditions in 0.5 min and maintained for 1.5 min.

261 The mass spectrometer ionization source was operated in positive mode. The
262 capillary and fragmentation voltages were 4000 and 100 V, respectively, the nebulizer
263 pressure was 40 psi, and the temperature was 350 °C. The triple quadrupole mass
264 spectrometer acquired data in multiple reactions monitoring mode.

265 **3. Results and discussion**

266 **3.1 Electrochemical Filter Design and Characterization**

267 The schematic of the MWCNTs-based electrochemical filter was presented in Fig.
268 1a and b. MWCNTs filter was operated anodically and was electrically connected via
269 a perforated stainless steel wire. Another perforated stainless wire was connected to
270 the DC power supply and was operated as the cathode. An insulating silicone rubber
271 O-ring was used to separate the electrodes, and another insulating silicone rubber
272 O-ring was used to densify the setup [44]. Fig. 1c presents the section of the
273 MWCNTs membrane, which was about 20 µm thick and exhibited stacked layers
274 structure with an effective filtration area of 706 mm².

275 Current - Voltage (*I* - *V*) curves for sodium chloride electrolyte solutions can be
276 found in Fig. 2 the change curves of the transient current with applied voltage and
277 current in NaCl solution with different concentrations at a flow rate of 1.5 mL/min
278 were drawn. At the same concentration, the current increased with increasing voltage.
279 At all voltage conditions, as the concentration increased, the current also increased.
280 When NaCl was added, the current increased linearly with the potential above 2.0 V.
281 This is related to the one-electron oxidation of chlorine: $\text{Cl}^- + \text{e}^- \rightarrow \text{Cl}\cdot$ [44] ($E^\circ = 2.4$
282 V). The NaCl concentration at 20 mmol/L was selected in the whole experiments.

283 **3.2 Removal efficiencies of antibiotics using different methods**

284 Both MWCNTs-based adsorptive filtration and electrochemical degradation can
285 remove antibiotics. Fig. 3 compares the breakthrough plots for the removal of SMZ
286 (Fig. 3a), CIP (Fig. 3b), and AMO (Fig. 3c). The three kinds of antibiotics used three
287 different methods including MWCNTs-based adsorptive filtration, electrochemical
288 degradation without MWCNTs membrane and MWCNTs-based electrochemical
289 membrane filtration. For SMZ, the adsorptive filtration efficiency was only 20% after
290 60 min, and electrochemical degradation efficiency was achieved at 75% after 60 min,
291 while MWCNTs-based electrochemical membrane filtration efficiency reached 90%
292 after 60 min. At time < 12 min, the efficiency of MWCNTs-based electrochemical
293 membrane filtration was lower to the adsorptive filtration, suggesting that an
294 electrostatic desorption occurred. Fig. 3b shows three kinds of removal efficiency for
295 CIP. The adsorptive filtration efficiency was only 5% after 60 min, and
296 electrochemical degradation efficiency was achieved at 60% after 60 min, while
297 MWCNTs-based electrochemical membrane filtration efficiency reached 76% after 60
298 min. At time < 18 min, the efficiency of MWCNTs-based electrochemical membrane
299 filtration was lower than the adsorptive filtration. At time < 28 min, the efficiency of
300 MWCNTs-based electrochemical membrane filtration was lower than electrochemical
301 degradation, indicating that electrostatic desorption occurred when the voltage was
302 applied. The results indicated that the absorption ability was suppressed when electric
303 field was applied in the system. Fig. 3c shows the adsorptive filtration efficiency for
304 AMO was only 13% after 60 min, and electrochemical degradation efficiency was
305 achieved at 94% after 60 min, while MWCNTs-based electrochemical membrane
306 filtration efficiency reached 98% after 60 min.

307 The physical sorption and the electrolysis were two major applied forces in the
308 experiments, and the latter usually played a leading role [45]. When both physical
309 sorption and the electrolysis simultaneously worked, the degradation efficiency of
310 antibiotics was the best.

311 Fig. 4a shows the adsorption breakthrough curve, $C_{\text{eff}}/C_{\text{in}}$ versus T , in the absence
312 of electricity for three kinds of antibiotics. In all cases, the concentration of the
313 antibiotics in the effluent was below the limitation of detection prior to breakthrough,

314 indicating that all antibiotic molecules collided with the surface of the MWCNTs as
315 they passed through the filter, causing them to be absorbed. The rapid adsorption can
316 be attributed to its relatively strong van der Waals, π - π , and cation- π interactions
317 with the *sp*²-conjugated MWCNTs [39]. Results showed that AMO was removed
318 more quickly than SMZ and CIP. It also showed that the adsorption rate for AMO was
319 higher than SMZ and CIP, and it was also much more exhausted than others. The
320 absorption capacities for AMO, SMZ and CIP were 6.47, 5.52 and 1.49 mg/g,
321 respectively. Due to the thin film properties of the filter, the total removal capacity of
322 the MWCNTs filter was relatively low compared to other membrane filtration
323 (displayed in Table S1). As shown in Fig. 4b, AMO was the easiest to be electrolyzed,
324 followed by SMZ and CIP. Noticeably, the removal efficiency for CIP was higher than
325 SMZ at the time less than 30 min, nevertheless, the removal efficiency for CIP was
326 lower than SMZ at the time more than 30 min owing to the different structures.
327 According to Fig. 4c, after an hour of MWCNTs-based electrochemical membrane
328 filtration, AMO was almost completely degraded, followed by SMZ (90%) and CIP
329 (76%). Compared to other electrochemical membrane filtration, it also showed
330 excellent degradation efficiencies (displayed in Table S2).

331 3.3 Effects of cell voltage

332 The degradation efficiencies of SMZ, AMO and CIP at four different applied
333 voltages (i.e., 0, 1, 2 and 3 V) using MWCNTs-based electrochemical membrane
334 filtration were investigated (displayed in Fig. 5). Results showed that the steady-state
335 effluent concentrations were achieved after 30 min, 50 min and 15 min for SMZ, CIP
336 and AMO, respectively. Moreover, the removal efficiencies increased with the
337 increasing voltage for all the antibiotics, which indicated that a stronger electric field
338 resulted in more efficient degradation. Fig. 5a shows the results of electrochemical
339 filtration of SMZ. It was noted that SMZ degradation efficiency at 1 V was nearly
340 identical to that at 0 V, indicating that the voltage was too low to activate the
341 production of reactive species on the surface of the MWCNTs anode. The removal
342 efficiencies were 70% and 90% at 2 and 3V, respectively. The absence of SMZ
343 breakthrough at 2 and 3V suggested that the main SMZ loss mechanism was

344 oxidation. Fig. 5b shows the influence voltages on CIP removal efficiency. Results
345 showed that the removal efficiency at 1V was similar to that at 0V, and the removal
346 efficiency at 2V was similar to that at 3V. Fig. 5c shows that the application of 1V
347 results in a slight decay in AMO breakthrough as compared to 0V conditions. The
348 removal efficiencies for AMO were >82% and >98% at 2 and 3 V, respectively. The
349 results were similar to SMZ and CIP electrochemical filtration results. Compared to
350 the application of 0 V, the slight improvement observed at 1 V was attributed to
351 electrostatic attraction thus enhancing mass transfer by migration from bulk to surface
352 [46]. However, compared to the application of 1V, an obvious degradation was taking
353 place at both 2 and 3 V. As the voltage increased, the number of generated electrons
354 increased, the content of free radicals increased, and the removal rate of contaminants
355 increased [39]. There is a conjugation effect and van der Waals force between
356 antibiotics and MWCNTs, and the adsorption force is stronger. When the voltage is
357 applied, the degradation rate of these antibiotics were greatly increased [47].

358 Overall, rapid removal of antibiotics in aqueous solution occurs when the
359 charging voltage exceeded 2 V, and removal was inefficient when the voltage was
360 decreased to 1 V. For MWCNTs based electrochemical membrane filtration,
361 antibiotics remaining in the solution followed pseudo-first-order decay during the
362 experiment (Eq. (1)).

$$363 \ln\left(\frac{c_t}{c_0}\right) = -k_{app}t \quad (1)$$

364 It was consistent with study of Zheng et al [49]. Apparent rate constants for
365 antibiotics removal (k_{app}) as a function of voltage applied are shown in Table 1. A
366 higher voltage led to a higher of the value of k_{app} . When the voltage was 3 V, the
367 degradation velocity of these antibiotics was AMO (0.061 s^{-1}) > SMZ (0.035 s^{-1}) >
368 CIP (0.023 s^{-1}). k_{app} at 0 V and 1 V were the same order of magnitude, k_{app} at 2 V
369 and 3 V were the same order of magnitude. For example, k_{app} at 2 V and 3 V were
370 10 times of the 0 V and 1 V.

371 3.4 Different concentrations of antibiotics

372 The WWTPs concentration was far above at ppb level, even reaching ppm level.

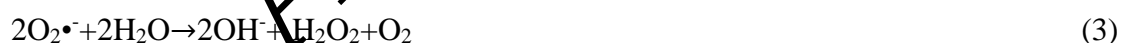
373 Therefore, three different concentrations (5 mg/L, 25 mg/L and 50 mg/L) of
374 antibiotics were tested to investigate the degradation performance. Fig. 6 illustrates
375 the removal efficiency of these antibiotics at different initial concentrations. It was
376 observed that the removal efficiency of SMZ, CIP and AMO decreased from 90%, 75%
377 and 99% to 51%, 43% and 16%, respectively, with the initial concentration of
378 antibiotics increased from 5 mg/L to 50 mg/L. It is due to the fact that the same
379 filtration volume and operating conditions of the electro-catalytic membrane, the
380 amount of $\bullet\text{OH}$ generation should be constant. Therefore, at higher initial
381 concentrations, the limited and constant $\bullet\text{OH}$ does not destroy much more antibiotic
382 and its intermediates [48]. Hence, this appliance could adapt to pollution with low
383 concentration and achieved high degradation efficiency. It could potentially be applied
384 in practical antibiotic wastewater treatment.

385 3.5 Effects of pH and temperature

386 The pH and temperature are factors that affect the electrochemical degradation of
387 the membrane. Raising the temperature can decrease the solution viscosity and
388 increase the mass transport rate from solution to the membrane surface, which will
389 promote to generate more electrons and free radical, thus, much more $\bullet\text{OH}$ will be
390 produced to degrade antibiotics as well as its intermediates. The pH is considered an
391 important factor since it mostly affects the speciation of the pollutants and the redox
392 potential of the generated oxidant.

393 In order to elucidate whether these antibiotics can be effectively degraded in a
394 wide pH range, electrochemical membrane filtration degradation of these antibiotics
395 was conducted under five pH conditions (i.e., pH = 3, 5, 7, 9 and 11). As shown in Fig.
396 7, removal efficiencies for SMZ and AMO were almost independent on pH values.
397 SMZ and AMO removal efficiencies were high and remain almost constant. However,
398 electrochemical membrane filtration degradation of CIP was strongly pH-dependent.
399 The removal efficiency under acidic or alkaline environment was higher than that
400 under neutral environment. The reason may be that target contaminant (i.e., SMZ, CIP
401 and AMO) in the solution had different forms at different pH value (see Fig. 8), thus
402 affecting the degradation mechanism of the pollutants [49, 50]. For SMZ, when pH <

403 pK_{a1} , the target contaminant was protonated and the molecule was positively charged,
404 which prevented the unshared pair electrons delocalizing from N atom to aromatic
405 ring and reduced their reactivity to electrophilic free radicals. When $pH > pK_{a2}$, -NH
406 sulfonamide group deprotonated could reduce electron withdrawing effect on the
407 aniline group, which enhanced its ability to radical oxidative activity [51]. It is well
408 known that $\bullet OH$ was an electron-deficient group belonging to an electrophile that
409 attacked a negatively charged molecule [51]. Eq. (2) and (3) shows that superoxide
410 anions ($O_2^{\bullet -}$) would be favorably stable at a neutral to alkaline pH, the removal
411 efficiency increased with a higher pH. While at an acidic pH, the formation of
412 hydrogen peroxide (H_2O_2) would be favored [38]. Notably, when the pH of the
413 solution decreased, the oxidation efficiency on the electrode surface decreased, and
414 thereby enhanced the oxidation capacity of the system. In addition, low pH values
415 also enhanced the effect of Cl^- on the removal efficiency of target pollutants, despite
416 the low concentration of Cl^- in wastewater. When the pH value was 3, the main active
417 chlorine substance was Cl_2 . From pH 3 to 8, the dominant species was $HClO$. Because
418 $HClO$ ($E^\circ = 1.49$ V/SHE) and Cl_2 ($E^\circ = 1.36$ V/SHE) showed higher oxidation
419 reduction potential than ClO^- ($E^\circ = 0.89$ V/SHE), there was no doubt that the reaction
420 in acidic solution can also be performed [52]. Therefore, whether it is acidic, neutral
421 or basic, the removal efficiency can get to a decent state.



422 **Temperature is associated with effluent treatment performance.** In general, the
423 removal efficiency increased with the increase of environment temperature, which
424 was due to the increase in the adsorption and oxidation load [36]. As illustrated in the
425 Fig. 9, increasing temperature could accelerate the degradation of contaminants. For
426 example, SMZ removal efficiency was 77%, 90%, 96% at the temperature of 15 °C,
427 25 °C, 35 °C, respectively. Increasing the temperature could reduce the viscosity of
428 the solution, thus increasing the mass transfer rate of the solution to the membrane
429 surface, and generating more electrons and holes [40]. Therefore, more $\bullet OH$ would
430 be produced to degrade antibiotics and their intermediates. The effect of temperature

431 on degradation efficiencies for these antibiotics was in the order SMZ > CIP > AMO.

432 **3.6 Effects of SDBS**

433 SDBS, a typical representative of anionic surfactant, was widely used to increase
434 the dispersity and stability of MWCNTs, and was selected as a model dissolved
435 natural organic matter due to the prevalence of substances in surface water and
436 wastewater effluent [53]. In our experiments, electrochemical membrane filtration
437 process was conducted with the SDBS concentration of 5 mg/L. Results showed that
438 antibiotics degradation in the presence of 5 mg/L SDBS was 7%, 8% and 1% lower
439 than that without SDBS for SMZ, CIP and AMO, respectively (shown in Fig. 10).
440 Among the targeted pollutants including AMO, SMZ and CIP, SDBS has the most
441 significant effect on the degradation of CIP while it exhibited the weakest effect on
442 AMO. This could be due to the specific molecular structure of SDBS. On the one
443 hand, the strong π - π electron-donor-acceptor interaction between the benzene ring of
444 SDBS molecule and the MWCNTs could compete for the absorption sites. On the
445 other hand, the hydrophobic tail (12-carbon alkyl chain) of SDBS may be bound to
446 the surface of MWCNTs through hydrophobic attraction. Song et al pointed out that
447 the adsorption capacity of sediment for SDBS was enhanced as a result of the
448 incorporation of MWCNTs [54]. So there may be a competitive relationship between
449 SDBS and these antibiotics.

450 **3.7 Reusability of membrane**

451 Antibiotics may accumulate in the channels of the MWCNTs during degradation
452 process, thus causing severe membrane fouling. MWCNTs-based electrochemical
453 filter membrane fouling was monitored by conducting four cycles of degradation
454 experiments to examine the reusability of the filter membrane. All cycles were carried
455 out with the same conditions (20 mM NaCl, 1.5 mL/min, 60 min). As shown in Fig.
456 11, the degradation efficiencies gradually decreased for all the three kinds of
457 antibiotics after each cycle of reuse. Noticeably, the removal efficiency was only 65%,
458 60% and 90% at the 4th cycle for SMZ, CIP and AMO, respectively, which exhibited
459 72%, 79% and 92% degradation performance for SMZ, CIP and AMO, respectively,
460 when compared to the first cycle. Among them, AMO had the highest degradation

461 efficiency. The loss of degradation efficiency was probably attributed to the high
462 molar mass products formed during SMZ and CIP oxidation as described later, which
463 could accumulate and jam the membrane access and bring about higher mass transfer
464 resistance [24]. The degradation ability of these antibiotics was: AMO>SMZ>CIP.
465 This result indicated that the MWCNTs membrane had excellent reusability for
466 electrochemical degradation, and this membrane has potential for practical
467 applications.

468 **3.8 Effects of simultaneous removal of SMZ, CIP, and AMO**

469 Under the optimal parameter conditions in electric filtration, the removal of
470 mixed contamination experiments was conducted to determine the combined removal
471 effects. As illustrated in Fig. 12, this group of experiments was divided into four
472 categories. In Fig. 12a, binary mixtures of SMZ and AMO were decomposed
473 simultaneously, AMO was nearly completely removed, and SMZ was only removed
474 60% within 60 min. SMZ and CIP were also degraded simultaneously (shown in Fig. 12b,
475 12b.). Results showed that both SMZ and CIP were nearly completely removed within
476 60 min. Nevertheless, the effluent concentrations of CIP and AMO binary solution
477 were both remained 12% after 60 min (displayed in Fig. 12c). Ternary systems were
478 also investigated in which SMZ, CIP and AMO were simultaneously added to the
479 apparatus (shown in Fig. 12d). Results showed that SMZ and AMO could be removed
480 thoroughly, while CIP was only removed 20%. In the experiments, SMZ, CIP and
481 AMO can be simultaneously removed at different degree. It was supposed that
482 degradation of AMO was the most simple owing to its structure, the next was SMZ,
483 the most difficult to be removed was CIP. Different molecular configuration led to
484 different electrochemical filtration behaviors. From the perspective of chemical
485 structure, AMO lactam ring was easily affected by external chemical environment,
486 such as acid, alkali, heat, nucleophile attack, which was prone to degradation by
487 opening loop [55]. In addition, multiple chiral centers and unsaturated double bonds
488 made AMO were prone to isomerization [56]. Moreover, some chemical structures of
489 the side chains were also prone to degradation or isomerization [7]. Considering the
490 different molecular structures, the discrepancy in the degradation between SMZ and

491 CIP can be explained. Since SMZ was comprised of benzene and isoxazole ring with
492 chain linkage whereas CIP had piperazine and quinolone ring connected by short
493 connection, the electron density of SMZ was expected to be lower than CIP [57]. In
494 this system, $\bullet\text{OH}$ played a more important role in SMZ and CIP oxidation. A
495 theoretical calculation indicated that the N-S bond, C-N bond, C-S bond, and the C-C
496 bond (benzene ring) in SMZ molecule, were easily broken by the attack of $\bullet\text{OH}$ [58],
497 while another calculation shows that the reaction site of $\bullet\text{OH}$ attack CIP was C-F
498 bond, C-N bond and C-C bond (benzene ring) [59]. Thus, compared to SMZ, CIP
499 degradation by MWCNTs-based electrochemical membrane filtration was found to be
500 less efficient.

501 3.9 Identification of transformation by-products

502 There are 11 intermediates had been detected through LC-MS analysis during
503 SMZ degradation by electrochemical membrane filtration. All intermediates
504 compounds identified were given in Table 2a and proposed a possible oxidation
505 mechanism. The main reaction pathways were summarized in Fig. 13a.

506 The first pathway was the oxidation of amino groups of benzene ring and the
507 formation of the nitro-derivative of SMZ. Compound C1 yielded an m/z ratio of 284.
508 There was a large body of literature that indicated that the amino group was oxidized
509 to nitro [60-62]. Then the opening of the isoxazole ring was assessed by identifying
510 compound C2. Afterwards, the loss of one carbonyl group generated the intermediate
511 C3 at the m/z of 246. It was obvious that the mass spectrum C3 increased significantly
512 at 40 minutes and decreased at 60 minutes, indicating that it was a characteristic
513 intermediate product. Due to the strong electron-withdrawing effect of the nitro group,
514 the nitro group was conjugated to the benzene ring, then the link between the benzene
515 ring and the sulfur disconnected, so compound C4 was gained. The second pathway
516 involved the attack of the hydroxyl radical on the isoxazole ring and then the
517 substitution of the amino group by a hydroxyl group in the benzene ring, which was at
518 the m/z of 271 (C5), which was in line with the previous reports [63]. Then owing to
519 the attack of $\bullet\text{OH}$ radicals to the double bond on the isoxazole ring, the
520 dihydroxylated compound C6 was formed. This intermediate was the same as C3,

521 with a maximum yield of 40 minutes and a decrease of 60 minutes, suggesting that the
522 pathway was reliable. The opening of the isoxazole ring and taking out one molecule
523 of carbonyl was figured out by recognizing compound C7. Ultimately, compound C8
524 was formed at the m/z of 140. The third pathway was that, the sulfonamide S-N bond
525 of SMZ was readily cleaved by the attack of oxidizing species, leading to the
526 formation of C9. **As to the formation of C10 at the m/z of 118 was due to the attack of**
527 **\bullet OH radicals, and the formation of C11 at the m/z of 179, similar intermediates had**
528 **also been identified in photocatalytic degradation reported by Ioannidou et al [60].**

529 Judging from the identified by-products, the following reaction pathways for CIP
530 degradation were proposed (shown in Fig. 13b). There were 12 intermediates that had
531 been detected through LC-MS analysis during CIP degradation by our methods. All
532 intermediates compounds identified were given in Table 2b and a possible oxidation
533 mechanism was proposed.

534 Degradation was mainly due to two reasons. On one hand, oxidation of
535 quinolones occurred thus leading to defluorination and hydroxyl substitution reactions.
536 On the other hand, the reaction at the piperazinyl ring was taken place [64]. The
537 similar degradation mechanism was also proposed by some studies using either
538 electrochemical oxidation or activated-persulfate degradation [65-67]. In our work,
539 both mechanisms described above were put forward simultaneously. Reaction at the
540 stepwise oxidative degradation of the piperazinyl side chain was found 10 kinds of
541 compounds. The oxidation of the piperazinyl led to ring opening, generating the
542 di-aldehyde derivative m/z 362 C4. Then, the degradation was continued in two ways.
543 The loss of one formaldehyde group of the piperazinyl group after oxidation to obtain
544 two isomers C5, and the other was defluorination on the quinolone group to obtain C6.
545 Then the piperazinyl group gradually removed the formaldehyde group to obtain C7
546 and C8, respectively, followed by the loss of formaldehyde from amine side chain to
547 obtain C9. The secondary pathway was the self-sensitized oxidation of quinolone ring,
548 followed by decarbonization and N-dealkylation on piperazine ring, and product C1
549 was obtained. The third pathway appeared to take place via the addition of two
550 oxygen atom that produced the dihydroxy derivative of piperazinyl ring (C2), and

551 then with another hydroxyl radical addition to the parent molecule get C3. The fourth
552 pathway was the intermediate product, C10, resulted from hydroxyl radical attacking
553 at the fluorine atom, followed by the hydroxylation resulting in the formation of C11
554 and C12, successively.

555 Analysis by LC-MS allowed the detection and identification of 7 intermediates
556 during AMO degradation. All intermediates compounds identified were given in Table
557 2c and a possible oxidation mechanism was proposed. The main reactions pathways
558 were summarized in Fig. 13c.

559 Degradation was mainly owing to three kinds of reasons. The first was due to the
560 fracture of the β -lactam ring, the second was due to the oxidation of sulfur atom, and
561 the third was cracked at the aromatic [68-70]. In our research, the first pathway began
562 with the attack of oxidants (e.g., $\text{HO}\cdot$, $\text{Cl}\cdot$) on sulfur atom of AMO, resulting in the
563 formation and hydroxylation of the sulfoxide derivatives (C1) and successively
564 forming complex compound (C2). Another pathway was initialized by the destruction
565 of the four-membered β -lactam ring, thus yielding the penicilloic acid (C3), which
566 contained a free carboxylic acid group. Decarboxylation of the free carboxylic acid
567 occurred and generated the intermediate C4. The third degradation pathway was
568 formed by the cleavage of AMO molecules on peptide bonds closer to the aromatic
569 ring to form p-hydroxybenzoic acid (C5) and a dicyclopentane product C6. Then C6
570 was degraded into an open chain structure (C7).

571 3.10 The electrochemical filtration mechanism

572 The organic electrochemical filtration reaction mechanism followed a multi-step
573 process: firstly, deposition and adsorption of antibiotics onto the electrode surface (Ep.
574 (4)). Secondly, antibiotics degraded and molecular transformed. The electrochemical
575 filter degradation of antibiotics may occur through two primary mechanisms, the
576 direct oxidation of antibiotics in contact with MWCNTs anode, and the indirect
577 oxidation of antibiotics through anodic production of some aqueous oxidants (e.g.,
578 $\text{HO}\cdot$, $\text{Cl}\cdot$) [18, 32, 33, 36, 37, 71]. These antibiotics degradation mechanisms were
579 shown in Fig. 14. Direct oxidation was the oxidation of antibiotics adhered to the
580 MWCNTs electrochemical filter, which was an electron process (Ep. (5)). Indirect

581 oxidation possessed two steps. The first step produced some solvated radicals on the
582 anode (Ep. (6)). The second step was that antibiotics were oxidized by the produced
583 oxidants step by step (Ep. (7)). According to the previous research, when anodic
584 potential < 0.8 V, direct oxidation played the main role in the system, once the anodic
585 potential was increased to > 0.95 V, the effluent concentration began to decrease with
586 increasing potential indicating that indirect and direct oxidation occurred
587 simultaneously [39]. Thirdly, the degradation product exfoliated. In addition, the
588 degradation of antibiotics partly might be caused by electrocoagulation due to the
589 dissolution of the porous stainless steel.



590 In order to determine the effect of the indirect pathway on the electrochemical
591 oxidation of antibiotics on MWCNTs electrode, the relevant experiments were
592 conducted by adding appropriate radical scavengers. Tertiary butanol (TBA) with
593 concentration of 5 mM was used as the HO• radicals scavenger and 5 mM
594 benzoquinone (BQ) was used as O₂•⁻ radicals scavenger. As shown in Fig. 15, SMZ
595 removal efficiency decreased 27.6% by adding TBA while it decreased 10.3% by
596 adding BQ, CIP removal efficiency decreased 25.1% by adding TBA while it
597 decreased 7.5% by adding BQ, AMO removal efficiency decreased 12.3% by adding
598 TBA while it decreased 5.2% by adding BQ, which meant that the HO• radicals
599 accounted for the primary role of indirect electrochemical oxidation for antibiotics
600 degradation and the effect of O₂•⁻ radical just played subsidiary role.

601 4. Conclusions

602 In this work, three kinds of antibiotics including SMZ, CIP and AMO were
603 simultaneously removed in binary and ternary systems using electrochemical filter.
604 The main conclusions were as follows: 1) MWCNTs-based electrochemical
605 membrane filtration comprised of a composite conductive electrochemical filter

606 membrane anode and a stainless steel network cathode. 2) After 60 min of
607 electrochemical filtration process, in single system, degradation of SMZ, CIP and
608 AMO was 90%, 76% and 98%, respectively. In both binary and ternary systems,
609 degradation efficiencies were in the order of AMO > SMZ > CIP. 3) Degradation
610 efficiency was enhanced by increasing the voltage and temperature, while it decreased
611 with the increased initial concentration and the addition of SDBS. The degradation
612 efficiencies of SMZ and AMO were independent on solution pH. However, the
613 degradation efficiency of CIP was higher in acidic or alkaline than that in neutral
614 solution. It still exhibited good antibiotics degradation efficiency after four time
615 cycles reuse. 4) Hydroxylation, cleavage of sulfonamide S-N bond and oxidation of
616 aniline moiety were found to be the major pathways, which was responsible for SMZ
617 degradation. The oxidation of quinolone ring and the reaction of the piperazinyl ring
618 were the major pathways of CIP. The fracture of the β -lactam ring, the oxidation of
619 sulfur atom and the crack at the aromatic were the reasons of AMO degradation. 5)
620 Both direct oxidation and indirect oxidation affected the degradation of antibiotics. In
621 summary, MWCNTs-based electrochemical membrane filtration was successful in
622 degrading multiple antibiotics and this study offers a promising technology to lessen
623 the hazardous effects of multiple antibiotics in nature.

625 Acknowledgements

626 The authors are grateful for the financial supports from National Natural Science
627 Foundation of China (51521006, 51579095 and 51378190), Natural Science
628 Foundation of Hunan Province, China (Grant No.2018JJ3053), the Program for
629 Changjiang Scholars and Innovative Research Team in University (IRT-13R17) and
630 The Three Gorges Follow-up Research Project(2017HXXY-05).

632 References:

- 633 [1] C. Zhang, D. Tian, X. Yi, T. Zhang, J. Ruan, R. Wu, C. Chen, M. Huang, G. Ying, Occurrence,
634 distribution and seasonal variation of five neonicotinoid insecticides in surface water and sediment of
635 the Pearl Rivers, South China, *Chemosphere* 217 (2019) 437-446.
636 [2] K. He, Z. Zeng, A. Chen, G. Zeng, R. Xiao, P. Xu, Z. Huang, J. Shi, L. Hu, G. Chen, Advancement

637 of Ag–Graphene Based Nanocomposites: An Overview of Synthesis and Its Applications, *Small* 14
638 (2018) 1800871.

639 [3] X. Yi, C. Zhang, H. Liu, R. Wu, D. Tian, J. Ruan, T. Zhang, M. Huang, G. Ying, Occurrence and
640 distribution of neonicotinoid insecticides in surface water and sediment of the Guangzhou section of
641 the Pearl River, South China, *Environ Pollut* 251 (2019) 892-900.

642 [4] S. Ye, M. Yan, X. Tan, J. Liang, G. Zeng, H. Wu, B. Song, C. Zhou, Y. Yang, H. Wang, Facile
643 assembled biochar-based nanocomposite with improved graphitization for efficient photocatalytic
644 activity driven by visible light, *Applied Catalysis B: Environmental* (2019).

645 [5] W. Wang, P. Xu, M. Chen, G. Zeng, C. Zhang, C. Zhou, Y. Yang, D. Huang, C. Lai, M. Cheng, L.
646 Hu, W. Xiong, H. Guo, M. Zhou, Alkali Metal-Assisted Synthesis of Graphite Carbon Nitride with
647 Tunable Band-Gap for Enhanced Visible-Light-Driven Photocatalytic Performance, *ACS Sustainable*
648 *Chemistry & Engineering* 6 (2018) 15503-15516.

649 [6] B. Qingwei, W. Bin, H. Jun, D. Shubo, Y. Gang, Pharmaceuticals and personal care products in the
650 aquatic environment in China: A review, *Journal of Hazardous Materials* 262C (2013) 189.

651 [7] I.T. Carvalho, L. Santos, Antibiotics in the aquatic environments: A review of the European scenario,
652 *Environment International* 94 (2016) 736-757.

653 [8] Z. Qian-Qian, Y. Guang-Guo, P. Chang-Gui, L. You-Sheng, Z. Jian-Liang, Comprehensive
654 evaluation of antibiotics emission and fate in the river basins of china: source analysis, multimedia
655 modeling, and linkage to bacterial resistance, *Environmental Science & Technology* 49 (2015)
656 6772-6782.

657 [9] R. Gothwal, T. Shashidhar, Antibiotic Pollution in the Environment: A Review, *CLEAN - Soil, Air,*
658 *Water* 43 (2015) 479-489.

659 [10] S. Suzuki, P.T. Hoa, Distribution of quinolones, sulfonamides, tetracyclines in aquatic
660 environment and antibiotic resistance in indochina, *Frontiers in Microbiology* 3 (2012) 67.

661 [11] S. Ye, G. Zeng, H. Wu, C. Zhang, J. Liang, J. Dai, Z. Liu, W. Xiong, J. Wan, P. Xu, Co-occurrence
662 and interactions of pollutants, and their impacts on soil remediation—A review, *Critical reviews in*
663 *environmental science and technology* 47 (2017) 1528-1553.

664 [12] Z.H. Wen, L. Chen, X.Z. Meng, Y.P. Duan, Z.S. Zhang, E.Y. Zeng, Occurrence and human health
665 risk of wastewater-derived pharmaceuticals in a drinking water source for Shanghai, East China,
666 *Science of the Total Environment* 490 (2014) 987-993.

667 [13] V. Homem, L. Santos, Degradation and removal methods of antibiotics from aqueous matrices – A
668 review, *Journal of Environmental Management* 92 (2011) 2304-2347.

669 [14] K.J. Choi, S.G. Kim, S.H. Kim, Removal of antibiotics by coagulation and granular activated
670 carbon filtration, *J Hazard Mater* 151 (2008) 38-43.

671 [15] Y. Yang, C. Zhang, C. Lai, G. Zeng, D. Huang, M. Cheng, J. Wang, F. Chen, C. Zhou, W. Xiong,
672 BiOX (X= Cl, Br, I) photocatalytic nanomaterials: applications for fuels and environmental
673 management, *Advances in colloid and interface science* 254 (2018) 76-93.

674 [16] L. Zhang, J. Zhang, G. Zeng, H. Dong, Y. Chen, C. Huang, Y. Zhu, R. Xu, Y. Cheng, K. Hou,
675 Multivariate relationships between microbial communities and environmental variables during
676 co-composting of sewage sludge and agricultural waste in the presence of PVP-AgNPs, *Bioresource*
677 *technology* 261 (2018) 10-18.

678 [17] H. Wang, Z. Zeng, P. Xu, L. Li, G. Zeng, R. Xiao, Z. Tang, D. Huang, L. Tang, C. Lai, Recent
679 progress in covalent organic framework thin films: fabrications, applications and perspectives,
680 *Chemical Society Reviews* 48 (2019) 488-516.

681 [18] P. Liu, H. Zhang, Y. Feng, C. Shen, F. Yang, Integrating electrochemical oxidation into forward
682 osmosis process for removal of trace antibiotics in wastewater, *Journal of Hazardous Materials* 296
683 (2015) 248-255.

684 [19] F. Sopaj, M.A. Rodrigo, N. Oturan, F.I. Podvorica, J. Pinson, M.A. Oturan, Influence of the anode
685 materials on the electrochemical oxidation efficiency. Application to oxidative degradation of the
686 pharmaceutical amoxicillin, *Chemical Engineering Journal* 262 (2015) 286-294.

687 [20] S.O. Ganiyu, N. Oturan, S. Raffy, M. Cretin, R. Esmilaire, E. van Hullebusch, G. Esposito, M.A.
688 Oturan, Sub-stoichiometric titanium oxide (Ti₄O₇) as a suitable ceramic anode for electrooxidation of
689 organic pollutants: A case study of kinetics, mineralization and toxicity assessment of amoxicillin,
690 *Water Res* 106 (2016) 171-182.

691 [21] M. Panizza, A. Dirany, I. Sirés, M. Haidar, N. Oturan, M.A. Oturan, Complete mineralization of
692 the antibiotic amoxicillin by electro-Fenton with a BDD anode, *Journal of Applied Electrochemistry* 44
693 (2014) 1327-1335.

694 [22] V. Homem, L. Santos, Degradation and removal methods of antibiotics from aqueous matrices – A
695 review, *Journal of Environmental Management* 92 (2011) 2304 - 2347.

696 [23] B.G. Padilla-Robles, A. Alonso, S.A. Martínez-Delgado, M. González-Brambila, U.J.
697 Jauregui-Haza, J. Ramirez-Munoz, Electrochemical degradation of amoxicillin in aqueous media,
698 *Chemical Engineering and Processing* 94 (2015) 93-98.

699 [24] C. Ji, J. Hou, V. Chen, Cross-linked carbon nanotubes-based biocatalytic membranes for
700 micro-pollutants degradation: Performance, stability, and regeneration, *Journal of Membrane Science*
701 520 (2016) 869-880.

702 [25] Y.F. Wang, H.O. Huang, X.M. Wei, Influence of wastewater pre-coagulation on adsorptive filtration
703 of pharmaceutical and personal care products by carbon nanotube membranes, *Chemical Engineering*
704 *Journal* 333 (2018) 66-75.

705 [26] M. Liu, Y. Liu, D. Bao, G. Zhu, G. Yang, J. Geng, H. Li, Effective Removal of Tetracycline
706 Antibiotics from Water using Hybrid Carbon Membranes, *Scientific Reports* 7 (2017) 43717.

707 [27] Y.F. Wang, J.X. Zhu, H.C. Huang, H.H. Cho, Carbon nanotube composite membranes for
708 microfiltration of pharmaceutical and personal care products: Capabilities and potential mechanisms,
709 *Journal of Membrane Science* 479 (2015) 165-174.

710 [28] H. Wu, X.J. Ni, J. Yang, C.H. Wang, M.Q. Lu, Retentions of bisphenol A and norfloxacin by
711 three different ultrafiltration membranes in regard to drinking water treatment, *Chemical Engineering*
712 *Journal* 294 (2016) 410-416.

713 [29] J. Lee, S. Jeong, Y. Ye, V. Chen, S. Vigneswaran, T. Leiknes, Z.W. Liu, Protein fouling in carbon
714 nanotubes enhanced ultrafiltration membrane: Fouling mechanism as a function of pH and ionic
715 strength, *Separation and Purification Technology* 176 (2017) 323-334.

716 [30] A.R. Bakr, M.S. Rahaman, Electrochemical efficacy of a carboxylated multiwalled carbon
717 nanotube filter for the removal of ibuprofen from aqueous solutions under acidic conditions,
718 *Chemosphere* 153 (2016) 508-520.

719 [31] J.-L. Gong, B. Wang, G.-M. Zeng, C.-P. Yang, C.-G. Niu, Q.-Y. Niu, W.-J. Zhou, Y. Liang,
720 Removal of cationic dyes from aqueous solution using magnetic multi-wall carbon nanotube
721 nanocomposite as adsorbent, *Journal of hazardous materials* 164 (2009) 1517-1522.

722 [32] Z. Pan, C. Song, L. Li, H. Wang, Y. Pan, C. Wang, J. Li, T. Wang, X. Feng, Membrane technology
723 coupled with electrochemical advanced oxidation processes for organic wastewater treatment: Recent
724 advances and future prospects, *Chemical Engineering Journal* (2019).

725 [33] S.O. Ganiyu, E.D. van Hullebusch, M. Cretin, G. Esposito, M.A. Oturan, Coupling of membrane
726 filtration and advanced oxidation processes for removal of pharmaceutical residues: A critical review,
727 Separation and Purification Technology 156 (2015) 891-914.

728 [34] Z.Z. Chowdhury, S. Sagadevan, R. Bin Johan, S.T. Shah, A. Adebisi, S. IslamMd, R.F. Rafique, A
729 review on electrochemically modified carbon nanotubes (CNTs) membrane for desalination and
730 purification of water, Materials Research Express 5 (2018) 102001.

731 [35] G. Gao, C.D. Vecitis, Doped Carbon Nanotube Networks for Electrochemical Filtration of
732 Aqueous Phenol: Electrolyte Precipitation and Phenol Polymerization, ACS Applied Materials &
733 Interfaces 4 (2012) 1478-1489.

734 [36] H. Liu, C.D. Vecitis, Reactive Transport Mechanism for Organic Oxidation during
735 Electrochemical Filtration: Mass-Transfer, Physical Adsorption, and Electron-Transfer, Journal of
736 Physical Chemistry C 116 (2016) 374-383.

737 [37] C.D. Vecitis, M.H. Schnoor, M.S. Rahaman, J.D. Schiffman, M. Elimelech, Electrochemical
738 multiwalled carbon nanotube filter for viral and bacterial removal and inactivation, Environmental
739 Science & Technology 45 (2011) 3672-3679.

740 [38] A.R. Bakr, M.S. Rahaman, Removal of bisphenol A by electrochemical carbon-nanotube filter:
741 Influential factors and degradation pathway, Chemosphere 185 (2017) 879-887.

742 [39] L. Yanbiao, L. Han, Z. Zhi, W. Tianren, O. Choon Nam, C.D. Vecitis, Degradation of the Common
743 Aqueous Antibiotic Tetracycline using a Carbon Nanotube Electrochemical Filter, Environmental
744 Science & Technology 49 (2015) 7974-7980.

745 [40] L. Zhimeng, Z. Mengfu, W. Zheng, W. Hong, D. Cheng, B. Ku, Effective Degradation of Aqueous
746 Tetracycline Using a Nano-TiO₂/Carbon Electrocatalytic Membrane, Materials.

747 [42] C. Trellu, C. Coetsier, J.C. Rouch, R. Esmilaire, M. Rivallin, M. Cretin, C. Causserand,
748 Mineralization of organic pollutants by anodic oxidation using reactive electrochemical membrane
749 synthesized from carbothermal reduction of TiO₂, Water Res 131 (2018) 310-319.

750 [43] A.M. Zaky, B.P. Chaplin, Mechanism of *p*-Substituted Phenol Oxidation at a Ti₄O₇ Reactive
751 Electrochemical Membrane, Environmental Science & Technology 48 (2014) 5857-5867.

752 [43] C. Trellu, C. Coetsier, J.C. Rouch, R. Esmilaire, M. Rivallin, M. Cretin, C. Causserand,
753 Mineralization of organic pollutants by anodic oxidation using reactive electrochemical membrane
754 synthesized from carbothermal reduction of TiO₂, Water Res 131 (2018) 310-319.

755 [44] C.D. Vecitis, G. Gao, H. Liu, Electrochemical Carbon Nanotube Filter for Adsorption, Desorption,
756 and Oxidation of Aqueous Dyes and Anions, The Journal of Physical Chemistry C 115 (2011)
757 3621-3629.

758 [45] Z. Niu, Y. Wang, H. Lin, F. Jin, Y. Li, J. Niu, Electrochemically enhanced removal of
759 perfluorinated compounds (PFCs) from aqueous solution by CNTs-graphene composite electrode,
760 Chemical Engineering Journal 328 (2017) 228-235.

761 [46] A.R. Bakr, M.S. Rahaman, Electrochemical efficacy of a carboxylated multiwalled carbon
762 nanotube filter for the removal of ibuprofen from aqueous solutions under acidic conditions,
763 Chemosphere 153 (2016) 508-520.

764 [47] L. Ji, W. Chen, S. Zheng, Z. Xu, D. Zhu, Adsorption of sulfonamide antibiotics to multiwalled
765 carbon nanotubes, Langmuir the Acs Journal of Surfaces & Colloids 25 (2009) 11608.

766 [48] X. Zhou, S. Liu, A. Xu, K. Wei, W. Han, J. Li, X. Sun, J. Shen, X. Liu, L. Wang, A multi-walled
767 carbon nanotube electrode based on porous Graphite-RuO₂ in electrochemical filter for pyrrole
768 degradation, Chemical Engineering Journal 330 (2017) 956-964.

769 [49] H. Chen, B. Gao, H. Li, L.Q. Ma, Effects of pH and ionic strength on sulfamethoxazole and
770 ciprofloxacin transport in saturated porous media, *Journal of contaminant hydrology* 126 (2011) 29-36.
771 [50] E.S. Elmolla, M. Chaudhuri, Degradation of amoxicillin, ampicillin and cloxacillin antibiotics in
772 aqueous solution by the UV/ZnO photocatalytic process, *Journal of hazardous materials* 173 (2010)
773 445-449.
774 [51] Y. Fan, Y. Ji, D. Kong, J. Lu, Q. Zhou, Kinetic and mechanistic investigations of the degradation
775 of sulfamethazine in heat-activated persulfate oxidation process, *Journal of hazardous materials* 300
776 (2015) 39-47.
777 [52] Y. Zhang, T. Yu, W. Han, X. Sun, J. Li, J. Shen, L. Wang, Electrochemical treatment of anticancer
778 drugs wastewater containing 5-Fluoro-2-Methoxypyrimidine using a tubular porous electrode
779 electrocatalytic reactor, *Electrochimica Acta* 220 (2016) 211-221.
780 [53] Y. Tian, B. Gao, K.J. Ziegler, High mobility of SDBS-dispersed single-walled carbon nanotubes in
781 saturated and unsaturated porous media, *Journal of Hazardous Materials* 186 (2011) 1766-1772.
782 [54] B. Song, P. Xu, G. Zeng, J. Gong, X. Wang, J. Yan, S. Wang, P. Zhang, W. Cao, S. Ye, Modeling
783 the transport of sodium dodecyl benzene sulfonate in riverine sediment in the presence of multi-walled
784 carbon nanotubes, *Water Research* 129 (2018) 20-28.
785 [55] A. Deshpande, K. Baheti, N. Chatterjee, Degradation of β -lactam antibiotics, *Current science*
786 (2004) 1684-1695.
787 [56] A. Yada, S. Okajima, M. Murakami, Palladium-Catalyzed Intramolecular Insertion of Alkenes into
788 the Carbon-Nitrogen Bond of β -Lactams, *Journal of the American Chemical Society* 137 (2015)
789 8708-8711.
790 [57] Y. Ji, C. Ferronato, A. Salvador, X. Yang, J.-M. Chovelon, Degradation of ciprofloxacin and
791 sulfamethoxazole by ferrous-activated persulfate: implications for remediation of groundwater
792 contaminated by antibiotics, *Science of the Total Environment* 472 (2014) 800-808.
793 [58] J. Yang, Z. Li, H. Zhu, Adsorption and photocatalytic degradation of sulfamethoxazole by a novel
794 composite hydrogel with visible light irradiation, *Applied Catalysis B: Environmental* 217 (2017)
795 603-614.
796 [59] Y. Wang, C. Shen, M. Zhang, B.-T. Zhang, Y.-G. Yu, The electrochemical degradation of
797 ciprofloxacin using a SnO₂-Sb/Ti anode: influencing factors, reaction pathways and energy demand,
798 *Chemical Engineering Journal* 296 (2016) 79-89.
799 [60] E. Ioannidou, Z. Kontistis, M. Antonopoulou, D. Venieri, I. Konstantinou, D.I. Kondarides, D.
800 Mantzavinos, Solar photocatalytic degradation of sulfamethoxazole over tungsten – Modified TiO₂,
801 *Chemical Engineering Journal* (2016).
802 [61] W.Q. Guo, R.L. Yin, X.J. Zhou, J.S. Du, H.O. Cao, S.S. Yang, N.Q. Ren, Sulfamethoxazole
803 degradation by ultrasound/ozone oxidation process in water: kinetics, mechanisms, and pathways,
804 *Ultrasonics Sonochemistry* 22 (2015) 182-187.
805 [62] Y. Ji, Y. Fan, K. Liu, D. Kong, J. Lu, Thermo activated persulfate oxidation of antibiotic
806 sulfamethoxazole and structurally related compounds, *Water Research* 87 (2015) 1-9.
807 [63] A.G. Trovó R.F. Nogueira, A. Agüera, A.R. Fernandezalba, C. Sirtori, S. Malato, Degradation of
808 sulfamethoxazole in water by solar photo-Fenton. Chemical and toxicological evaluation, *Water*
809 *Research* 43 (2009) 3922-3931.
810 [64] S.K. Mondal, A.K. Saha, A. Sinha, Removal of ciprofloxacin using modified advanced oxidation
811 processes: Kinetics, pathways and process optimization, *Journal of Cleaner Production* 171 (2018)
812 1203 - 1214.

- 813 [65] Y. Ji, C. Ferronato, A. Salvador, X. Yang, J.M. Chovelon, Degradation of ciprofloxacin and
814 sulfamethoxazole by ferrous-activated persulfate: Implications for remediation of groundwater
815 contaminated by antibiotics, *Science of the Total Environment* 472 (2014) 800-808.
- 816 [66] S. Li, J. Hu, Transformation products formation of ciprofloxacin in UVA/LED and UVA/LED/TiO
817 2 systems: Impact of natural organic matter characteristics, *Water Research* 132 (2018) 320.
- 818 [67] T. An, H. Yang, G. Li, W. Song, W.J. Cooper, X. Nie, Kinetics and mechanism of advanced
819 oxidation processes (AOPs) in degradation of ciprofloxacin in water, *Applied Catalysis B*
820 *Environmental* 94 (2010) 288-294.
- 821 [68] W. Guo, Q.-L. Wu, X.-J. Zhou, H.-O. Cao, J.-S. Du, R.-L. Yin, N.-Q. Ren, Enhanced amoxicillin
822 treatment using the electro-peroxone process: key factors and degradation mechanism, *RSC Advances*
823 5 (2015) 52695-52702.
- 824 [69] D. Klauson, J. Babkina, K. Stepanova, M. Krichevskaya, S. Preis, Aqueous photocatalytic
825 oxidation of amoxicillin, *Catalysis Today* 151 (2010) 39-45.
- 826 [70] A.G. Trovó, R.F.P. Nogueira, A. Ana, A.R. Fernandez-Alba, M. Sixto, Degradation of the
827 antibiotic amoxicillin by photo-Fenton process--chemical and toxicological assessment, *Water*
828 *Research* 45 (2011) 1394-1402.
- 829 [71] H. Liu, J. Liu, Y. Liu, K. Bertoldi, C.D. Vecitis, Quantitative 2D electrocatalytic carbon nanotube
830 filter model: Insight into reactive sites, *Carbon* 80 (2014) 651-664.

Accepted MS